CHEMISTRY OF MATERIALS
Article
pubs.acs.org/cm

Fluorination of Polythiophene Derivatives for High Performance Organic Photovoltaics

Jea Woong Jo,[†] Jae Woong Jung,[†] Hsin-Wei Wang,[‡] Paul Kim,[‡] Thomas P. Russell,[‡] and Won Ho Jo*[,†]

[†]Department of Materials Science and Engineering, Seoul National University, Gwanak-ro, Gwanak-gu, Seoul 151-744, Korea
[‡]Department of Polymer Science and Engineering, University of Massachusetts, Amherst, Massachusetts 01003, United States

Supporting Information

ABSTRACT: For the purpose of examining the tuning of photophysical property by fluorine atom substitution, fluorinated and nonfluorinated poly(3,4-dialkylterthiophenes) (PDATs) were synthesized, and their photovoltaic properties were compared. Fluorinated PDATs exhibit a deeper highest occupied molecular orbital energy level than nonfluorinated ones, leading to higher open-circuit voltage in organic solar cells and also enhanced molecular ordering as evidenced by a vibronic shoulder in UV−vis spectra, $\pi-\pi$ scattering in GIWAXS, and a well-developed fibril structure in TEM, which contributes to efficient charge transport. As a result, the fluorine substitution increases the power conversion efficiency by 20% to 250% as compared with nonfluorinated PDATs.

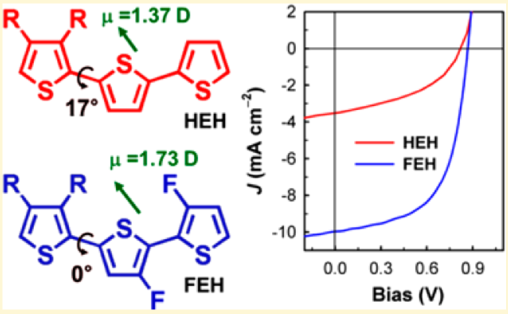

INTRODUCTION

For developing high efficiency organic photovoltaics (OPVs), understanding of the relation between chemical structure and photovoltaic property of semiconducting conjugated polymer (SCP) is essential. It has been reported that the electronic properties of SCPs can be tuned by modification of molecular structure such as atomic substitution,[1−4] optimization of length and position of alkyl chain,[5−7] introduction of bridge unit,[8−10] and type of chain end-group.[11,12] Among these methods, the atomic substitution, especially, the substitution of fluorine atom has attracted much attention for the past few years. It has recently been reported that fluorine substituted SCP-based solar cells exhibit high power conversion efficiencies (PCEs) over 7%.[13−16]

Fluorination has been known to cause multiple effects on photophysical properties of SCPs, and several possible explanations for improvement of solar cell performance by substitution of fluorine atom in SCPs have been proposed. First, since the fluorine atom has a strong electron-withdrawing nature, the substitution of fluorine on backbone of SCPs can lower the highest occupied molecular orbital (HOMO) energy level of SCPs and thereby enhance the open-circuit voltage (V_{OC}) of OPVs, because V_{OC} is proportional to the difference between the HOMO energy level of donor and the lowest unoccupied molecular orbital (LUMO) energy level of acceptor.[13,14] Second, the strong electronegativity of fluorine induces a strong dipole along the C−F bond, resulting in a strong inter/intramolecular interaction in SCP chains which influences the morphology of the active layer.[17−19] Third, the induced dipole may also accelerate exciton dissociation and increase the lifetime of charge carrier by reducing Coulombic interaction between electron and hole.[20,21]

In this work, we synthesized difluoro-bithiophene as a new building block for SCPs and polymerized with 3,4-dialkylterthiophene to afford fluorinated poly(3,4-dialkylterthiophene) (PDAT) in order to clarify the effect of fluorine atom substitution on the properties of SCPs and its device performance of OPVs. Considering that nonfluorinated PDATs exhibited a moderate PCE of 4.2% in OPVs in previous reports,[22,23] fluorinated PDATs synthesized in this work exhibit a higher PCE of 5.2% with a higher V_{OC} due to deeper HOMO energy levels than nonfluorinated PDATs and higher J_{SC} owing to enhanced molecular ordering with stronger dipole and better planarity, as evidenced by strong vibronic shoulder in UV−vis absorption spectra, $\pi-\pi$ scattering in grazing incidence wide angle X-ray scattering (GIWAXS), and a well-developed fibril structure in the active layer of OPVs, which is beneficial for transport of charge carriers. The fluorinated PDAT exhibits a promising PCE of 5.2%, which is 3.5 times higher than the corresponding nonfluorinated one, when a bulky group (ethylhexyl) was introduced as a side alkyl chain.

EXPERIMENTAL SECTION

Materials. 5,5′-Bis(trimethylsilyl)-3,3′-dibromo-2,2′-bithiophene,[24] 5,5′-bis(trimethyl-stannyl)-2,2′-bithiophene,[25] and 2,5-dibromo-3,4-didodecylthiophene (**6**)[22] were synthesized by following the methods reported in the literature. Poly(3,4-ethylenedioxy-thiophene):poly(styrenesulfonate) (PEDOT:PSS) (CleviosP VP AI 4083) was purchased from H. C. Stark and passed through a 0.45 μm PVDF syringe filter before spin-coating. [6,6]-Phenyl-C_{71}-butyric acid methyl ester ($PC_{71}BM$) was obtained from American Dye Source. All reagents

Received: May 1, 2014

dx.doi.org/10.1021/cm502229k | Chem. Mater. XXXX, XXX, XXX−XXX

were purchased from Sigma-Aldrich unless specified and used as received.

5,5′-Bis(trimethylsilyl)-3,3′-difluoro-2,2′-bithiophene (1). To 5,5′-bis(trimethylsilyl)-3,3′-dibromo-2,2′-bithiophene (2.5 g, 5.34 mmol) solution in anhydrous THF (25 mL) was added dropwise at −78 °C 2.5 M of *n*-BuLi in hexane (4.7 mL, 11.8 mmol). After having been stirred for 30 min, the solution was further stirred for 30 min at room temperature. The solution was then cooled to −78 °C again before *N*-fluorobenzenesulfonimide ($(PhSO_2)_2NF$) (4 g, 12.7 mmol) in THF (10 mL) was added. After having been warmed up to room temperature and stirred overnight, the resulting mixture was poured into water and extracted with diethyl ether. The organic phase was collected and dried over $MgSO_4$. The product was purified by column chromatography on silica gel (hexane as eluent) to yield the compound **1** as a white solid (1.65 g, 89%). ^1H NMR (300 MHz, $CDCl_3$): δ (ppm) 6.95 (s, 2H), 0.32 (s, 12H). ^{13}C NMR (300 MHz, $CDCl_3$): δ (ppm) 155.47 (d), 136.23 (d), 124.49 (d), 127.28 (dd), −8.14. *m/z* (MS-EI) calcd: 347, found: 346.

5,5′-Dibromo-3,3′-difluoro-2,2′-bithiophene (2). To a solution of compound **1** (2 g, 5.77 mmol) in chloroform/acetic acid (1/1, 20 mL) was added *N*-bromosuccinimide (NBS) (2.36 g, 13.3 mmol) in the dark. After stirring overnight at 60 °C, the reaction mixture was poured into water, extracted with chloroform, and dried over $MgSO_4$. Then the residue was purified by column chromatography on silica gel (hexane as eluent). Recrystallization from acetonitrile afforded the compound **2** (1.62 g, 78%). ^1H NMR (300 MHz, $CDCl_3$): δ (ppm) 6.87 (s, 2H). ^{13}C NMR (300 MHz, $CDCl_3$): δ (ppm) 152.01 (d), 120.12 (d), 112.37 (dd), 111.59 (d). *m/z* (MS-EI) calcd: 360, found: 360.

5,5′-Bis(trimethylstannyl)-3,3′-difluoro-2,2′-bithiophene (3). To the compound **2** (1.2 g, 3.33 mmol) in anhydrous THF (15 mL) was added dropwise at −78 °C 2.5 M of *n*-BuLi in hexane (3 mL, 7.5 mmol). After having been stirred for 30 min, the solution was further stirred for 30 min at room temperature. The solution was then cooled to −78 °C again before 1 M of trimethyltin chloride in hexane (8.3 mL, 8.3 mmol) was added. After having been warmed up to room temperature and stirred overnight, the resulting mixture was poured into water and extracted with diethyl ether. The organic phase was collected and dried over $MgSO_4$. Recrystallization from methanol yielded the compound **2** (1 g, 57%). ^1H NMR (300 MHz, $CDCl_3$): δ (ppm) 6.89 (t, 2H), 0.39 (m, 12H). ^{13}C NMR (300 MHz, $CDCl_3$): δ (ppm) 155.20 (d), 138.19 (d), 123.31 (d), 116.75 (dd), −0.38. *m/z* (MS-EI) calcd: 528, found: 528.

3,4-Bis(2-ethylhexyl)-thiophene (5). 3,4-Dibromothiophene (1 g, 4.13 mmol) was added to a mixture of 1 M of (2-ethylhexyl) magnesium bromide in diethyl ether (20 mL, 20 mmol) and a catalytic amount of $Ni(dppp)Cl_2$. After having been stirred at room temperature for 2 days, the solution was cooled to 0 °C, and 30 mL of 1 M HCl was added. Then, the organic phase was extracted with hexane and dried over $MgSO_4$. The product was purified by column chromatography on silica gel (hexane as eluent) to yield the compound **5** (0.55 g, 43%). ^1H NMR (300 MHz, $CDCl_3$): δ (ppm) 6.85 (s, 2H), 2.43 (d, 4H) 1.65−0.82 (m, 30H). ^{13}C NMR (300 MHz, $CDCl_3$): δ (ppm) 141.21, 120.74, 39.42, 33.28, 32.68, 28.93, 25.75, 23.11, 14.17, 10.85. *m/z* (MS-EI) calcd: 309, found: 308.

2,5-Dibromo-3,4-bis(2-ethylhexyl)-thiophene (7). To a solution of compound **5** (0.5 g, 1.62 mmol) in chloroform/acetic acid (1/1, 10 mL) was added NBS (0.72 g, 4.04 mmol) in the dark, and the solution was stirred overnight at 60 °C. After having been poured into water, the product was extracted with chloroform, washed with saturated $NaHCO_3$, and dried over $MgSO_4$. The product was purified by column chromatography on silica gel (hexane as eluent) to yield the compound **7** (0.65 g, 86%). ^1H NMR (300 MHz, $CDCl_3$): δ (ppm) 2.47 (d, 4H) 1.65−0.82 (m, 30H). ^{13}C NMR (300 MHz, $CDCl_3$): δ (ppm) 141.02, 108.58, 39.64, 33.42, 32.53, 28.89, 25.75, 23.12, 14.15, 11.11. *m/z* (MS-EI) calcd: 466, found: 466.

Synthesis of Polymers. The polymer H12 was synthesized by following the method reported in the literature.[22] The polymer HEH was synthesized as follows: the compound **5** (150 mg, 0.32 mmol) and 5,5′-bis(trimethylstannyl)-2,2′-bithiophene (157 mg, 0.57 mmol) were dissolved in a mixture of toluene (10 mL) and DMF (1 mL) solution. After the solution was flushed with N_2 for 20 min, 20 mg of $Pd(PPh_3)_4$ was added. The reaction mixture was stirred for 4 h at 150 °C in a microwave reactor, followed by end-capping using 2-bromothiophene and 2-tributyltinthiophene. After having been cooled to room temperature, the mixture was poured into methanol. The crude product was filtered through a Soxhlet thimble and then subjected to Soxhlet extraction with methanol, ethyl acetate, hexane, and chloroform. The polymer was recovered from chloroform fraction, and the fraction was precipitated into methanol to afford the product as a dark red solid (41 mg, 28%). The polymer F12 was synthesized as follows: The compounds **3** (288 mg, 0.55 mmol) and **6** (316 mg, 0.55 mmol) were dissolved in a mixture of toluene (15 mL) and DMF (1 mL) solution. After the solution was flushed with N_2 for 20 min, 20 mg of $Pd(PPh_3)_4$ was added. The reaction mixture was refluxed for 3 days, followed by end-capping using 2-bromothiophene and 2-tributyltinthiophene. After having been cooled to room temperature, the mixture was poured into methanol. The crude product was filtered through a Soxhlet thimble and then subjected to Soxhlet extraction with methanol, ethyl acetate, hexane, and chloroform. The polymer was recovered from chloroform fraction, and the fraction was precipitated into methanol to afford the product as a dark purple solid (93 mg, 27%). FEH was also synthesized by following the same procedure as used in the synthesis of F12. The compounds **3** (310 mg, 0.59 mmol) and **7** (280 mg, 0.59 mmol) were used as monomers, and a dark purple solid was obtained as a product (110 mg, 37%).

Characterization. The chemical structures of compounds were identified by ^1H NMR and ^{13}C NMR (Avance DPX-300). Molar masses of compounds were measured on a mass spectrometer (HP 5890) in electron-impact mode. Molecular weight and its distribution of polymers were measured by GPC (Polymer Laboratories GPC 220) with a refractive index detector at 135 °C. 1,2,4-Trichlorobenzene was used as an eluent, and the molecular weight of polymers was calibrated by polystyrene standards. The optical absorption spectra were obtained by a UV−vis spectrophotometer (Shimadzu UV-3600). Cyclic voltammetry was conducted on a potentiostat/galvanostat (VMP 3, Biologic) in an electrolyte solution of 0.1 M tetrabutylammonium hexafluorophosphate acetonitrile. Pt wires (Bioanalytical System Inc.) were used as both counter and working electrodes, and silver/silver ion (Ag in 0.1 M $AgNO_3$ solution, Bioanalytical System Inc.) was used as a reference electrode. The HOMO energy levels of polymers were calculated by using the flowing relation: HOMO (eV) $= -[E_{ox} - E_{1/2}(\text{ferrocene}) + 4.8]$, where E_{ox} is the onset oxidation potential of the polymer, and $E_{1/2}$(ferrocene) is the onset oxidation potential of ferrocene vs Ag/Ag^+. DFT calculations were carried out at the B3LYP/6-31G(d,p) level on Gaussian 03.

Device Fabrication and Testing. The polymer solar cells were fabricated with a device configuration of glass/ITO/PEDOT:PSS/polymer:$PC_{71}BM$/Ca/Al. PEDOT:PSS was spin-coated with 40 nm thickness on the ITO-coated glass and annealed at 150 °C for 30 min. The blend solution (2 wt %) of H12/$PC_{71}BM$, HEH/$PC_{71}BM$, and F12/PC71BM and a 3 wt % solution of FEH/$PC_{71}BM$ in *o*-dichlorobenzene were spin-coated on the top of the PEDOT:PSS layer at 700−1000 rpm for 40 s. The film thickness of the active layer was measured by surface profiler (AlphaStep IQ, KLA Tencor). Calcium (20 nm) and aluminum (100 nm) was thermally evaporated on the top of the active layer under vacuum ($<10^{-6}$ Torr). The effective area of the cell was ca. 0.06 mm^2. The current density−voltage (J−V) characteristics were measured with a Keithley 2400 source-meter under AM 1.5G (100 mW/cm^2) simulated by a Newport-Oriel solar simulator. The light intensity was calibrated using a NREL-certified photodiode prior to each measurement. The external quantum efficiency was measured using a lock-in amplifier with a current preamplifier under a short circuit current state with illumination of monochromatic light. The morphologies of polymer/$PC_{71}BM$ blend films were observed by a transmission electron microscope (TEM) (JEOL 2000 FX MARK II). The space charge limited current (SCLC) J−V curves were obtained in the dark using hole-only devices (ITO/PEDOT:PSS/polymer:$PC_{71}BM$/Au), and hole mobilities were calculated using the Mott−Gurney square law, $J = (9/8)\varepsilon_0\varepsilon_r\mu(V^2/L^3)$,

Scheme 1. Synthesis of Monomers and PDATs

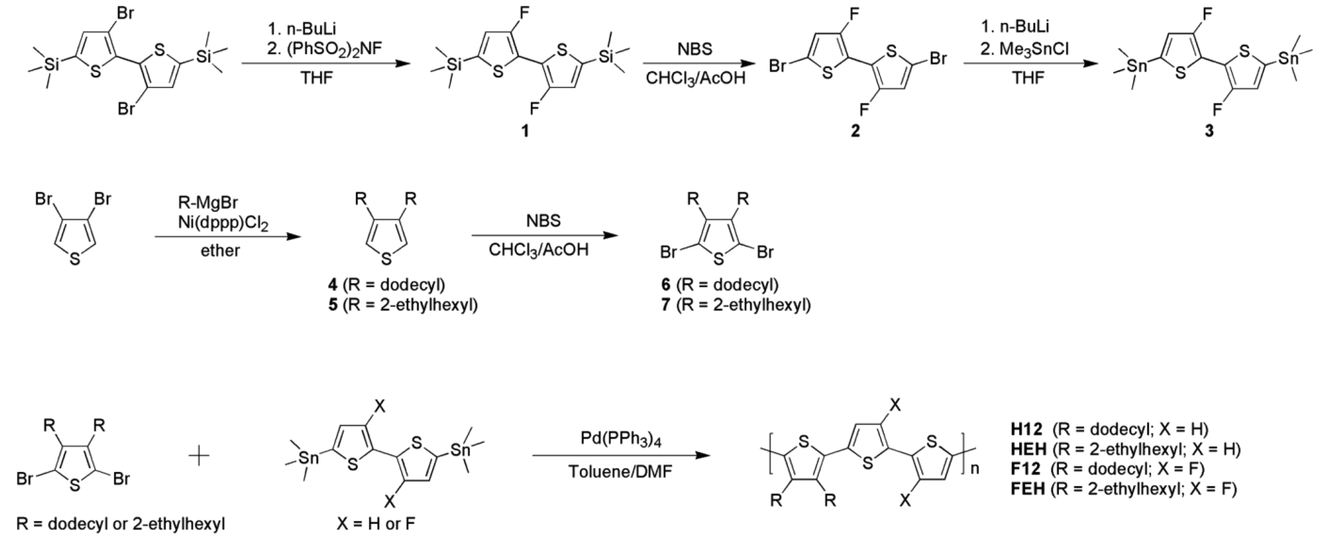

where ε_0 is vacuum permittivity, ε_r is the dielectric constant of polymer, μ is the charge carrier mobility, V is the effective applied voltage, and L is the thickness of the film. GIWAXS scans were obtained at the Advanced Light Source at the Lawrence Berkeley National Laboratory. The wavelength of X-ray used was 1.240 Å, and the scattered intensity was detected by a PILATUS 1 M detector. R-SoXS spectra were obtained using the transmission geometry with a beam energy of 284.2 eV.

■ RESULTS AND DISCUSSION

Synthesis and Characterization. The synthetic routes for monomers and polymers are illustrated in Scheme 1. Dodecyl or 2-ethylhexyl side chains were introduced to enhance the solubility of synthesized polymer in organic solvents. When shorter linear alkyl chains (hexyl or octyl) were introduced, fluorinated polymers exhibited poor solubility in organic solvents. Fluorinated bithiophene **1** was synthesized from 3,3′-dibromo-2,2′-bithiophene, electrophilic fluorination agent $(PhSO_2)_2NF$, and a trimethylsilane protecting group. Trimethylsilane groups in **1** were replaced by bromine to afford the compound **2**, and then the monomer **3** was synthesized through lithiation of the compound **2** with *n*-BuLi and subsequent quenching with trimethyltin chloride. Polymerization was carried out via the Stille coupling reaction in toluene/DMF with $Pd(PPh_3)_4$ as a catalyst. The molecular weights and polydispersity indexes (PDI) of polymers were measured by high temperature GPC and listed in Table 1.

Optical and Electrochemical Properties. The UV−vis absorption spectra of four polymers in chloroform solution and the film state are shown in Figure 1. In the film state, fluorinated polymers (F12 and FEH) show stronger vibronic shoulder at 598 nm than nonfluorinated polymers (H12 and HEH), indicating that the fluorine substitution enhances interchain interaction between polymers. Another interesting feature to note is that F12 exhibits a strong vibronic shoulder at 598 nm in solution, while FEH does not show the vibronic absorption, indicating that FEH is soluble in chloroform while F12 is not completely dissolved in the solvent. Therefore, a bulky side chain (ethylhexyl) is more effective to dissolve the fluorinated polymers. The optical bandgaps of all PDATs are nearly identical (∼1.95 eV) except FEH with a slightly lower bandgap. When electrochemical properties are measured by cyclic voltammetry, as shown in Figure 1c, the HOMO energy levels of fluorinated polymers (F12 and FEH) were around −5.41 eV, while those of the nonfluorinated polymers (H12 and HEH) are around −5.28 eV, as listed in Table 1. Hence, higher V_{OC} are expected in the devices fabricated from F12 and FEH. When the LUMO energy levels of polymers were estimated by adding the optical bandgap to the HOMO energy level, the LUMO energy levels of four polymers are in the range of −3.31 to −3.51 eV, which provides a sufficient LUMO level offset between polymers and PCBM (−4.0 eV) for effective exciton dissociation at the interface between donor and acceptor.[26]

Table 1. Characteristics of Polymers

PDAT	M_n [kg/mol]	PDI	$E_{g,opt}$[a] [eV]	HOMO [eV]	LUMO[b] [eV]
H12	14	1.38	1.95	−5.28	−3.33
HEH	12	1.73	1.96	−5.27	−3.31
F12	16	1.45	1.95	−5.40	−3.45
FEH	14	2.34	1.91	−5.42	−3.51

[a] Determined from the onset of UV−vis absorption spectra. [b] $E_{g,opt}$+HOMO.

Computational Simulation. To further understand the effect of fluorination on polymer properties, torsional angles, dipole moments, and orbital distribution of terthiophenes as model compounds were calculated using the density functional theory (DFT) (Figure 2 and Figure S1). Fluorinated terthiophene exhibits more planar structure than a nonfluorinated one, because the torsional angle at the minimum energy state of fluorinated terthiophene is 0° while the angle of the nonfluorinated one is 17°, as shown in Figure 2. The high planarity of the fluorinated polymer might come from increase of conjugation,[27] and the planar structure can improve intermolecular interaction of polymers with extended π-conjugation.[28] The fluorinated terthiophene has a higher dipole moment (1.73 D) than nonfluorinated terthiophene (1.37 D) (Figure S1b), and thus fluorinated PDAT is expected to exhibit a more closed packed structure because high dipole moment enhances molecular ordering.

Photovoltaic Properties. The photovoltaic properties were measured with the standard device configuration of ITO/PEDOT:PSS/polymer:$PC_{71}BM$/Ca/Al (Figure 3a) and

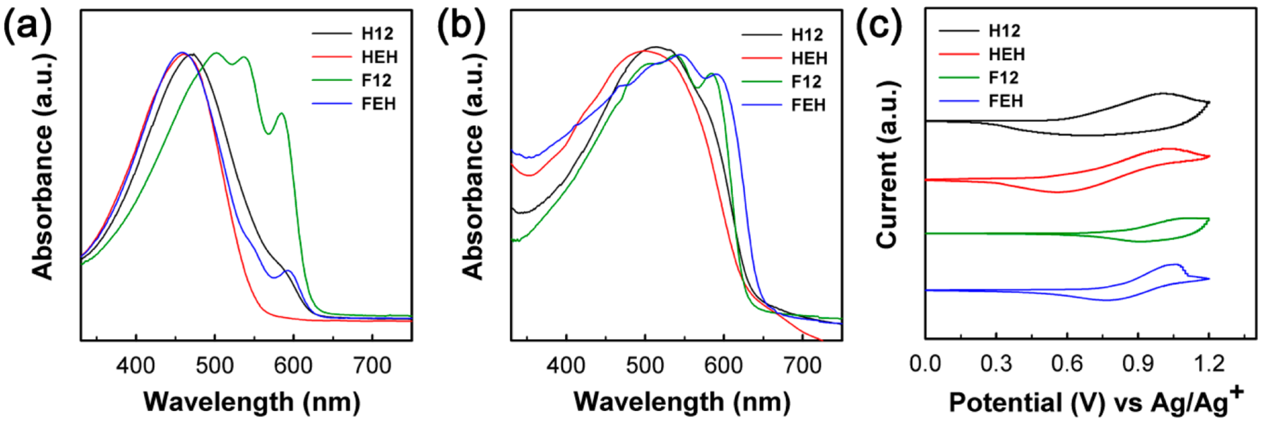

Figure 1. UV−vis absorption spectra of PDATs in (a) $CHCl_3$ solution and (b) film state; (c) cyclic voltammograms of PDATs.

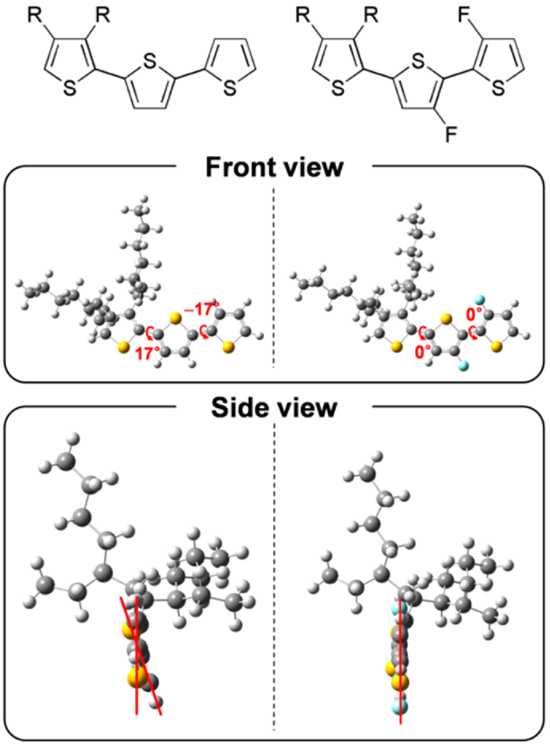

Figure 2. Torsion angle at the minimum energy state of nonfluorinated and fluorinated terthiophene (R = 2-ethylhexyl) calculated using DFT with a basis set of B3LYP/6-31G(d,p).

listed in Table 2. Since a deeper HOMO energy level of donor polymer affords higher V_{OC}, the V_{OC}s of fluorinated polymers are higher than those of the corresponding nonfluorinated polymers. Particularly, FEH shows a remarkably high V_{OC} over 0.87 V. As a result, the FEH-based device exhibits a promising PCE of 5.2% at the optimized film thickness of 140 nm, which is 3.5 times larger than the HEH-based device. Considering that the devices fabricated from the most commonly used polythiophene derivative in OPVs, poly(3-hexylthiophene), exhibit a V_{OC} of around 0.6 V,[29] the high V_{OC} of FEH-based device indicates that the photovoltaic properties of SCPs can be effectively controlled by fluorine substitution.

The external quantum efficiencies (EQEs) of devices were measured under monochromatic light (Figure 3b). Since the polymers have limited optical absorption with a bandgap of 1.95 eV, the EQEs over 650 nm arise from $PC_{71}BM$.[30] FEH exhibits EQE over 60% yielding in higher J_{SC}, while polymers with dodecyl side chain (H12 and F12) show EQEs below 40% in the wavelength range of 400−650 nm. When hole mobilities are estimated from dark J−V curve by using the space charge limited current (SCLC) model, as shown in Figure 3c, the SCLC hole mobility of FEH/$PC_{71}BM$ device is one order magnitude higher than those of the others (Table 2), indicating that the FEH/$PC_{71}BM$ blend provides a more effective charge pathway in an out-of-plane direction.[31,32] The preferential orientation of polymers was investigated by GIWAXS. All pristine polymer films show only (h00) reflections in the out-of-plane (q_z) direction, as shown in Figure 4, indicating that most of the polymer chains take edge-on orientation on the substrate. The (100) peaks of H12, HEH, F12, and FEH are observed at q_z = 0.24, 0.34, 0.31, and 0.44 Å^{-1}, respectively, corresponding to the interchain distance of 26.2, 18.5, 20.3, and 14.3 Å. The polymers with a shorter side chain (ethylhexyl) exhibit a shorter interchain distance than those with a longer side chain (dodecyl). It has also been observed that the interchain distances of fluorinated polymers are shorter than those of the corresponding nonfluorinated polymers, indicating that fluorinated polymers are more closely packed in ordered crystalline domain. Another important feature is that F12 and FEH clearly show the (010) reflection at q_{xy} = 1.7 Å^{-1} corresponding to the π−π stacking distance of 3.7 Å, as shown in Figure 4b, while nonfluorinated polymers do not exhibit discernibly the (010) reflection as also observed in a previous report.[22] This leads us to conclude that fluorination significantly enhances polymer chain packing in the π−π direction. It has also been observed that the FEH/$PC_{71}BM$ blend exhibits a weak (010) diffraction peak in the out-of-plane direction along with stronger (100) diffraction in the in-plane direction of GIWAXS as compared with the other blends, as shown in Figure 3d, indicating a part of FEH crystals take the face-on orientation after blending with $PC_{71}BM$, which may contribute to effective charge transport. It should be noted here that the (100) d-spacings of all polymer/$PC_{71}BM$ blends are the same as those of corresponding pristine polymers, implying that $PC_{71}BM$ molecules do not intercalate in between side chains of polymers.[32−34]

Morphology of Active Layer. Morphologies of active layers were observed by transmission electron microscopy (TEM), as shown in Figure 5. The active layer of H12/$PC_{71}BM$ shows a large phase separation between polymer and PCBM while that of HEH/$PC_{71}BM$ exhibits a homogeneously mixed morphology. The large domain sizes of H12/PCBM over 100

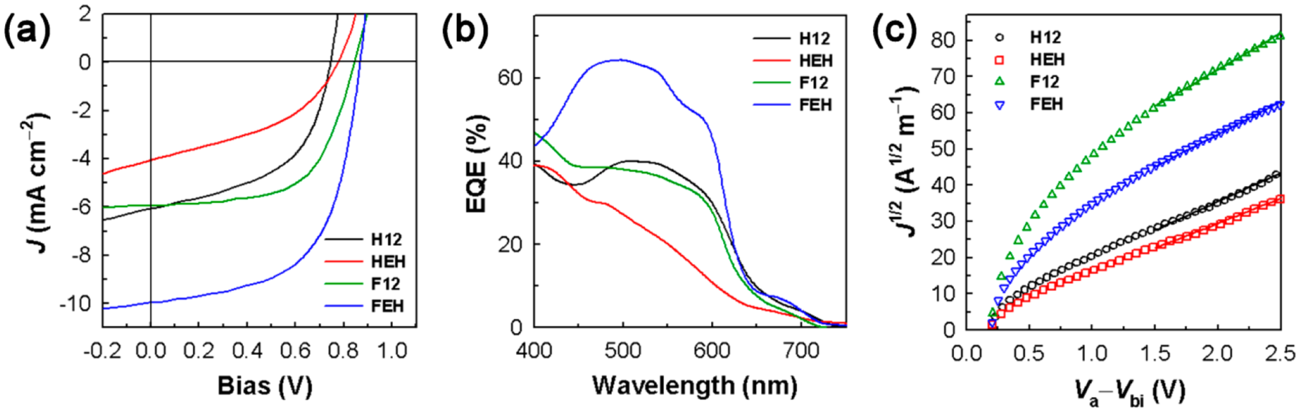

Figure 3. (a) $J-V$ curves and (b) EQE spectra of PDAT/PC$_{71}$BM solar cells; (c) dark $J-V$ characteristics of PDAT/PC$_{71}$BM blends with hole-only device, where the solid lines represent the best linear fit of the data points.

Table 2. Photovoltaic Properties of Devices under Standard AM 1.5G Illumination

PDAT	polymer: PC$_{71}$BM [w/w]	thickness [nm]	μ_h SCLC [cm^2/V s]	V_{OC} [V]	J_{SC} [mA/cm^2]	FF [%]	PCE$_{max}$ ($_{aver}$) [%]
H12	1:0.8	75	3.5×10^{-5}	0.77	6.09	53	2.49 (2.24)
HEH	1:0.8	70	2.2×10^{-5}	0.80	4.04	43	1.39 (1.18)
F12	1:1	80	6.3×10^{-5}	0.84	5.93	61	3.04 (2.86)
FEH	1:0.8	90		0.88	8.79	63	4.87 (4.64)
FEH	1:0.8	140	3.0×10^{-4}	0.87	9.82	61	5.20 (4.94)

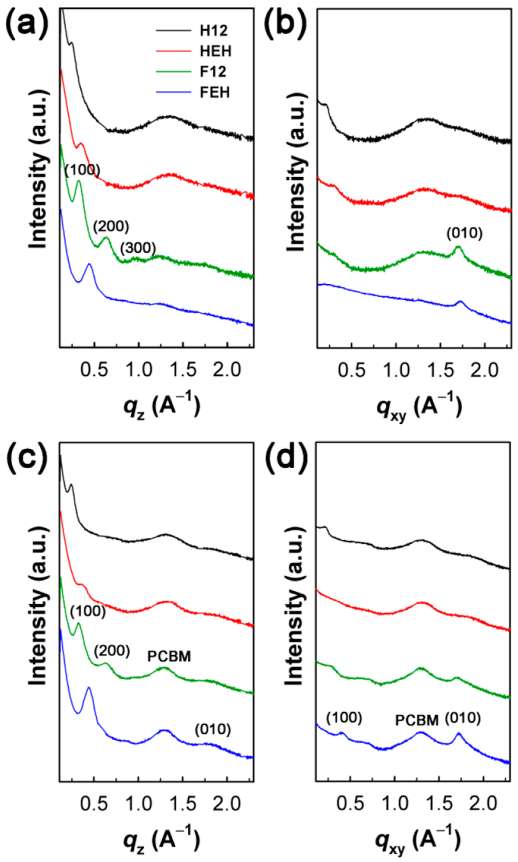

Figure 4. (a) q_z and (b) q_{xy} scans of GIWAXS from thin films of PDATs; (c) q_z and (d) q_{xy} scans of GIWAXS from blend films of PDAT/PC$_{71}$BM.

nm are not effective for charge generation because of limited exciton diffusion length (~10 nm) in OPVs.[35] However, the active layer of fluorinated polymer/PC$_{71}$BM shows a well-developed fibril structure, indicating improved ordering of polymer chains by fluorination which is beneficial for charge transport. Particularly, FEH with a bulky side chain exhibits finer fibrils than F12 with a linear side chain, as shown in Figure 5c and 5d, leading to higher J_{SC} due to a larger interface area between polymer and PCBM domains.

The transmission resonant soft X-ray scattering (R-SoXS) were measured at the carbon K absorption edge to determine the average domain size of the polymer/PCBM blend. The R-SoXS scattering profiles of four blends at the photon energy of 248.2 eV, where the contrast between PC$_{71}$BM and PDATs is the maximum, are shown in Figure 5e. The domain sizes of H12, HEH, F12, and FEH as determined from the peak of the profile are 310, 16, 190, 31 nm, respectively, which are very consistent with the sizes estimated from TEM images in Figure 5. It is also realized that polymers with bulky side chain have smaller domain sizes than those with linear side chains. In short, fluorination increases planarity of chains and thus enhances chain packing which contributes to the increase of J_{SC} and also lowers the HOMO energy level which increases the V_{OC} as compared to the nonfluorinated one.

■ CONCLUSION

We designed and synthesized polythiophene derivatives difluoro-bithiophene. Fluorination on polymer backbone changes its electronic structure, leading to a deeper HOMO energy level and enhances molecular packing of the polymers as evidenced by a strong vibronic shoulder in a UV−vis absorption spectrum and a $\pi-\pi$ stacking pattern in GIWAXS. When bulky side chains (ethylhexyl) are introduced as a solubilizing group, fluorinated polythiophenes develop a finer fibril structure and exhibit a promising PCE of 5.12% with a V_{OC} of 0.87 V and a J_{SC} of 9.82 mA cm^{-2}. Our results suggest that the photophysical properties and device performances of SCPs can be easily tuned by substitution of a fluorine atom on a polymer chain.

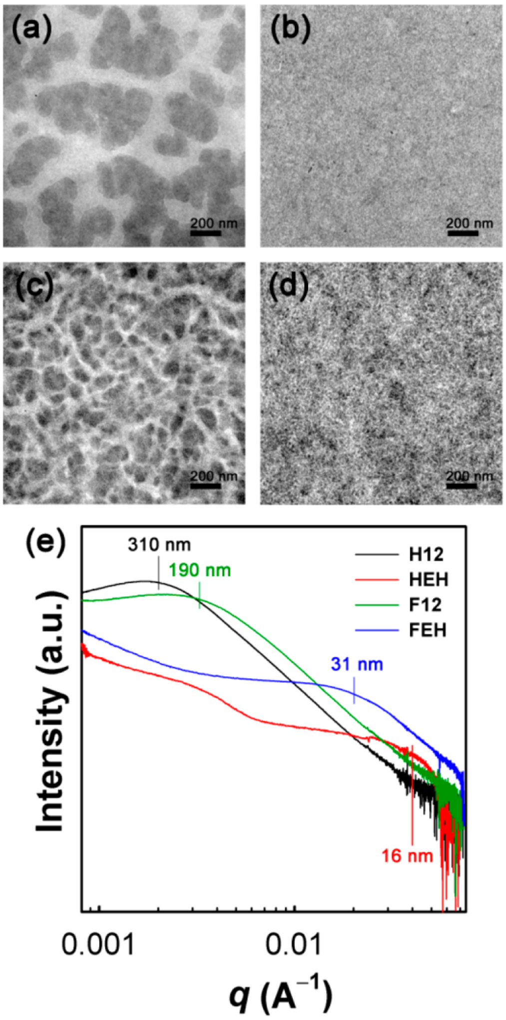

Figure 5. TEM images of PDAT/PC$_{71}$BM blend films: (a) H12, (b) HEH, (c) F12, and (d) FEH; (e) R-SoXS profiles of PDAT/PC$_{71}$BM blend films.

ASSOCIATED CONTENT

Supporting Information

Torsion potential energies and dipole moments of non-fluorinated and fluorinated terthiophene, GIWAXS pattern images, calculated HOMO and LUMO. This material is available free of charge via the Internet at http://pubs.acs.org.

AUTHOR INFORMATION

Corresponding Author

*E-mail: whjpoly@snu.ac.kr.

Notes

The authors declare no competing financial interest.

ACKNOWLEDGMENTS

The authors thank the Ministry of Education, Science and Technology (MEST), Korea for financial support through the Global Research Laboratory (GRL) program. T.P.R. also acknowledges the support from the U.S. Department of Energy through the Energy Frontier Research Center.

REFERENCES

(1) Blouin, N.; Michaud, A.; Gendron, D.; Wakim, S.; Blair, E.; Neagu-Plesu, R.; Belletete, M.; Durocher, G.; Tao, Y.; Leclerc, M. *J. Am. Chem. Soc.* **2008**, *130*, 732.

(2) Zhou, H. X.; Yang, L. Q.; Price, S. C.; Knight, K. J.; You, W. *Angew. Chem., Int. Ed.* **2010**, *49*, 7992.

(3) Hou, J. H.; Chen, H. Y.; Zhang, S. Q.; Li, G.; Yang, Y. *J. Am. Chem. Soc.* **2008**, *130*, 16144.

(4) Woo, C. H.; Beaujuge, P. M.; Holcombe, T. W.; Lee, O. P.; Frechet, J. M. J. *J. Am. Chem. Soc.* **2010**, *132*, 15547.

(5) Yang, L. Q.; Zhou, H. X.; You, W. *J. Phys. Chem. C* **2010**, *114*, 16793.

(6) Cabanetos, C.; El Labban, A.; Bartelt, J. A.; Douglas, J. D.; Mateker, W. R.; Frechet, J. M. J.; McGehee, M. D.; Beaujuge, P. M. *J. Am. Chem. Soc.* **2013**, *135*, 4656.

(7) Jung, J. W.; Jo, J. W.; Liu, F.; Russell, T. P.; Jo, W. H. *Chem. Commun.* **2012**, *48*, 6933.

(8) Lu, J. P.; Liang, F. S.; Drolet, N.; Ding, J. F.; Tao, Y.; Movileanu, R. *Chem. Commun.* **2008**, 5315.

(9) Zhou, E. J.; Yamakawa, S.; Zhang, Y.; Tajima, K.; Yang, C. H.; Hashimoto, K. *J. Mater. Chem.* **2009**, *19*, 7730.

(10) Fei, Z. P.; Shahid, M.; Yaacobi-Gross, N.; Rossbauer, S.; Zhong, H. L.; Watkins, S. E.; Anthopoulos, T. D.; Heeney, M. *Chem. Commun.* **2012**, *48*, 11130.

(11) Park, J. K.; Jo, J.; Seo, J. H.; Moon, J. S.; Park, Y. D.; Lee, K.; Heeger, A. J.; Bazan, G. C. *Adv. Mater.* **2011**, *23*, 2430.

(12) Lee, J. U.; Kim, Y. D.; Jo, J. W.; Kim, J. P.; Jo, W. H. *J. Mater. Chem.* **2011**, *21*, 17209.

(13) Chen, H. Y.; Hou, J. H.; Zhang, S. Q.; Liang, Y. Y.; Yang, G. W.; Yang, Y.; Yu, L. P.; Wu, Y.; Li, G. *Nat. Photonics* **2009**, *3*, 649.

(14) Zhou, H. X.; Yang, L. Q.; Stuart, A. C.; Price, S. C.; Liu, S. B.; You, W. *Angew. Chem., Int. Ed.* **2011**, *50*, 2995.

(15) Price, S. C.; Stuart, A. C.; Yang, L. Q.; Zhou, H. X.; You, W. *J. Am. Chem. Soc.* **2011**, *133*, 4625.

(16) Chang, C.; Zuo, L.; Yip, H.; Li, Y.; Li, C.; Hsu, C.; Cheng, Y.; Chen, H.; Jen, A. K.-Y. *Adv. Funct. Mater.* **2013**, *23*, 5084−5090, DOI: 10.1002/adfm201301557.

(17) Stuart, A. C.; Tumbleston, J. R.; Zhou, H. X.; Li, W. T.; Liu, S. B.; Ade, H.; You, W. *J. Am. Chem. Soc.* **2013**, *135*, 1806.

(18) Okamoto, T.; Nakahara, K.; Saeki, A.; Seki, S.; Oh, J. H.; Akkerman, H. B.; Bao, Z.; Matsuo, Y. *Chem. Mater.* **2011**, *23*, 1646.

(19) Yang, L. Q.; Tumbleston, J. R.; Zhou, H. X.; Ade, H.; You, W. *Energy Environ. Sci.* **2013**, *6*, 316.

(20) Carsten, B.; Szarko, J. M.; Son, H. J.; Wang, W.; Lu, L. Y.; He, F.; Rolczynski, B. S.; Lou, S. J.; Chen, L. X.; Yu, L. P. *J. Am. Chem. Soc.* **2011**, *133*, 20468.

(21) Rolczynski, B. S.; Szarko, J. M.; Son, H. J.; Liang, Y. Y.; Yu, L. P.; Chen, L. X. *J. Am. Chem. Soc.* **2012**, *134*, 4142.

(22) Ko, S. W.; Verploegen, E.; Hong, S.; Mondal, R.; Hoke, E. T.; Toney, M. F.; McGehee, M. D.; Bao, Z. *J. Am. Chem. Soc.* **2011**, *133*, 16722.

(23) Ko, S. W.; Hoke, E. T.; Pandey, L.; Hong, S. H.; Mondal, R.; Risko, C.; Yi, Y. P.; Noriega, R.; McGehee, M. D.; Bredas, J. L.; Salleo, A.; Bao, Z. *J. Am. Chem. Soc.* **2012**, *134*, 5222.

(24) Guo, X.; Puniredd, S. R.; Baumgarten, M.; Pisula, W.; Mullen, K. *J. Am. Chem. Soc.* **2012**, *134*, 8404.

(25) Fong, H. H.; Pozdin, V. A.; Amassian, A.; Malliaras, G. G.; Smilgies, D. M.; He, M. Q.; Gasper, S.; Zhang, F.; Sorensen, M. *J. Am. Chem. Soc.* **2008**, *130*, 13202.

(26) Brabec, C. J.; Gowrisanker, S.; Halls, J. J. M.; Laird, D.; Jia, S. J.; Williams, S. P. *Adv. Mater.* **2010**, *22*, 3839.

(27) Son, H. J.; Wang, W.; Xu, T.; Liang, Y.; Wu, Y.; Li, G.; Yu, L. *J. Am. Chem. Soc.* **2011**, *133*, 1885.

(28) Facchetti, A. *Chem. Mater.* **2011**, *23*, 733.

(29) Li, G.; Shrotriya, V.; Huang, J. S.; Yao, Y.; Moriarty, T.; Emery, K.; Yang, Y. *Nat. Mater.* **2005**, *4*, 864.

(30) Wienk, M. M.; Kroon, J. M.; Verhees, W. J. H.; Knol, J.; Hummelen, J. C.; van Hal, P. A.; Janssen, R. A. J. *Angew. Chem., Int. Ed.* **2003**, *42*, 3371.

(31) Piliego, C.; Holcombe, T. W.; Douglas, J. D.; Woo, C. H.; Beaujuge, P. M.; Frechet, J. M. J. *J. Am. Chem. Soc.* **2010**, *132*, 7595.

(32) Subramaniyan, S.; Xin, H.; Kim, F. S.; Shoaee, S.; Durrant, J. R.; Jenekhe, S. A. *Adv. Energy Mater.* **2011**, *1*, 854.

(33) Cates, N. C.; Gysel, R.; Beiley, Z.; Miller, C. E.; Toney, M. F.; Heeney, M.; McCulloch, I.; McGehee, M. D. *Nano Lett.* **2009**, *9*, 4153.

(34) Miller, N. C.; Cho, E.; Gysel, R.; Risko, C.; Coropceanu, V.; Miller, C. E.; Sweetnam, S.; Sellinger, A.; Heeney, M.; McCulloch, I.; Bredas, J. L.; Toney, M. F.; McGehee, M. D. *Adv. Energy Mater.* **2012**, *2*, 1208.

(35) Liu, F.; Gu, Y.; Jung, J. W.; Jo, W. H.; Russell, T. P. *J. Polym. Sci. Polym. Phys.* **2012**, *50*, 1018.